IEEE Access
Multidisciplinary | Rapid Review | Open Access Journal

Received September 10, 2018, accepted October 16, 2018. Date of publication xxxx 00, 0000, date of current version xxxx 00, 0000.

Digital Object Identifier 10.1109/ACCESS.2018.2879469

Estimating Water Current Velocities by Using a Model-Based High-Gain Observer for an Autonomous Underwater Vehicle

EONJOO KIM[1], SHUANGSHUANG FAN[1,2], (Member, IEEE), AND NEIL BOSE[1,2]

[1]Australian Maritime College, University of Tasmania, Launceston, TAS 7250, Australia
[2]Department of Ocean and Naval Architectural Engineering, Memorial University of Newfoundland, St. John's, NL A1C 5S7, Canada

Corresponding author: Shuangshuang Fan (shuangshuang.fan@utas.edu.au)

This work was supported by the Maritime Robotics Project (PI Neil Bose) from the Memorial University of Newfoundland, Canada. The work of E. Kim was supported by the Australian Postgraduate Award. The work of S. Fan was supported by the Startup Funds from the Australian Maritime College.

ABSTRACT For accurate control and navigation of an autonomous underwater vehicle (AUV) it is critical to know the water current velocities around the vehicle body. The AUV-onboard acoustic doppler current profilers are unable to measure the current near to the vehicle due to their blanking distance, so an AUV model-based observer can serve the purpose of estimating the current velocities surrounding the vehicle. In this paper, a high-gain observer based on an AUV dynamics model was used to estimate 3D water current velocities. The water current velocities were determined by calculating the differences between the vehicle velocities over the ground measured by a Doppler velocity log-aided inertial navigation system and the vehicle velocities through the water estimated by the model-based observer. Modeling and field trials of a Gavia AUV were used to demonstrate the approach. Instead of deriving the roll, pitch, and yaw motions, these were directly given as simulation inputs which allowed the AUV dynamics model to be simplified to 3–degrees of freedom. This paper presents a real-time model identification algorithm to identify the nonlinear parameters of the AUV model by utilizing a recursive least squares method. The real-time model identification algorithm allows the AUV model to be continuously updated in response to the operational environment. A high-gain observer was chosen as a nonlinear estimation algorithm to obtain the vehicle velocities through the water, and the Lyapunov stability of the estimation error dynamics was investigated. The observer gain was computed by solving the linear matrix inequality which represented the error dynamics. By utilizing the observer in the AUV dynamic model, the vehicle's velocity vector through the water was estimated, then the current velocity vector was calculated. In order to investigate the differences between the estimated current velocities and the measured current velocities, the standard deviations between these two were quantified. The results showed that the current estimation found by using the model-based observer was improved compared with the previous water current estimation method, which found the water velocity components in a turbulent water column from the AUV motion response.

INDEX TERMS Autonomous underwater vehicles, system identification, recursive least squares optimization, model-aided inertial navigation, linear matrix inequality, high-gain observer.

I. INTRODUCTION

AUVs have been used as specialised tools for ocean missions such as seabed observation, environmental monitoring and oceanographic measurement. These tasks involve high-resolution, georeferenced optical/acoustic ocean floor mapping as well as water column sampling such as currents, temperature and salinity [1]. Georeferencing is critical for AUVs to register navigational information and to revisit a previous mission site. Since the 1970s, the navigation and control subsystems of AUVs have been progressively and continuously improved. One of the major challenges is to achieve accurate localisation and navigation in regions where the DVL is out of range of the bottom [2].

Inertial navigation systems (INS) are one of the essential pieces of equipment used to localise and navigate AUVs. By utilising an Inertial Measurement Unit (IMU), the INS estimate the position, orientation and velocity of the vehicle relative to the inertial frame. However, a navigational system based solely on an INS has a relatively large position error drift and this can be reduced through an externally aided

bottom tracking DVL [3]. Furthermore, DVL aiding is either intermittently or completely unavailable when the vehicle-to-seabed distance is larger than the transmission range of DVL's acoustic frequency as illustrated in Figure 1. In this case, the vehicle's velocity can be approximated using a mathematical model which characterises the hydrostatics and hydrodynamic properties of the AUV; i.e. a model-aided INS [4]. Even though the localisation from the model-aided INS is not as precise as the DVL-aided INS, its accuracy is higher than an unaided INS and the water-track mode DVL-aided INS [5]. Therefore, this paper presents an approach to estimate the vehicle's velocity by using an AUV model-based observer for the case when the vehicle operates in the midwater zone or loses the bottom track due to very rough bathymetry in deep water.

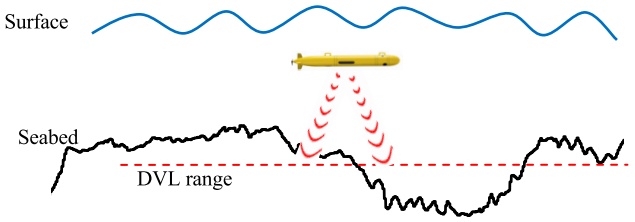

FIGURE 1. Illustration of an AUV temporarily operating beyond the DVL range.

The capability of a mathematical model for predicting AUV velocity depends on the accuracy of the parameters representing hydrodynamic, hydrostatic, environmental and external forces and the mass properties of the AUV. Since the hydrodynamic forces acting on AUVs are highly nonlinear, mathematical models should have high-order hydrodynamic coefficients to represent these nonlinear characteristics. Numerous methods for identifying linear and nonlinear hydrodynamic coefficients have been introduced for marine vehicles. For example, captive model experiments [6], computational fluid dynamics (CFD) simulation [7] and system identification utilising field experiment data [8].

In many cases it is necessary or useful to have a model of the system with the model coefficients available on-line in real time while the system is in operation. The model coefficients should be obtained based on the observations up to the current time. The on-line computation of the model coefficients must also be done in such a way that the processing of the measurements from one sample can be completed during one sampling interval. Otherwise the model computations cannot keep up with the information flow. Identification techniques that comply with this requirement will be called recursive identification methods, since the measured input-output data are processed recursively (sequentially) as they become available [9].

The linear and nonlinear parameters of an AUV motion response prediction mathematical model are presented here by utilising the Recursive Least Squares (RLS) and the prediction error method (PEM) optimisation techniques in Randeni *et al.* [2]. The difference between velocity prediction uncertainties of the models identified using the Recursive Least Squares (RLS) and PEM are negligibly small. That is, both identification algorithms are equally capable of estimating the parameters of the model. The determined velocities were used to aid the INS position estimate using a Kalman filter data fusion algorithm when external aiding was unavailable. The model is able to estimate the position of the AUV within an uncertainty range of around 1.5% of the distance travelled, significantly improving the localisation accuracy.

In addition to the prediction of the motion response, an AUV's mathematical model can also be used to calculate the water velocity components of a turbulent water column in three dimensions using the AUV's motion response [10]. The water column velocities are determined by calculating the differences between the motion responses of the vehicle in calm and turbulent water environments. In the Randeni, et al. [10] work, the calculated water column velocity components show good agreement with the current measurements from an ADCP mounted on the AUV.

In practice, perfect observation of the system state is unavailable, as either it is costly, technically unfeasible, or the measurement quality is low. Therefore, there is a need for a systematic approach for the evaluation or estimation of the system state using the information available. For a linear system, the idea that a stabilising controller can consist of a state estimator plus state feedback, called the separation principle, is a valid approach. However, for a nonlinear system, the separation principle does not hold since it is nearly impossible to estimate the error dynamics. Hence many nonlinear estimation algorithms have been developed such as the extended Kalman Filter (EKF) [11], unscented Kalman filter (UKF) [12], particle filter (PF) [13] and high-gain observer [14].

The high-gain observer distinguishes itself from other methods by its simple structure since it only consists of a copy of the system dynamics with a corrective term involving the product of the output observation error by the observer gain. As a result high-gain observers have been used extensively in the feedback control design for nonlinear systems; see Khalil and Praly [15] for example. The high-gain observer not only recovers stability achieved under state feedback, but also recovers its performance in the sense that the trajectories of the system under output feedback, approach those under state feedback as the observer gain increases [16], [17].

As ocean current or water column information might enhance navigation precision and control performance, current velocities were estimated by a nonlinear observer based on the AUV dynamic model in a current by Fan, et al. [18]. In the AUV dynamic model, the current was assumed to be composed of unsteady and nonuniform components. While the current disturbances were taken as the uncertainties of the vehicle dynamic system, a nonlinear observer was used to estimate the unmeasured state, which was fed back to the control system. However, as the most critical parameter, the observer gain matrix in Fan *et al.* [18] is preliminarily

optimized by utilising the pole placement method to place the eigenvalues of the closed-loop system in some desired regions of the complex plane, it is inferred that there is enormous room to improve the robustness and precision of the observer by adopting advanced algorithms to optimize the observer gain matrix.

The issue of selecting a high gain arises from the demand of accounting for the nonlinearities in the error dynamics which are typically represented as a Lipschitz function. Alessandri and Rossi [19] present a time-varying increasing-gain observer for a nonlinear system. In the first time instant, the gain is small, but it increases over time up to its maximum value and then is kept constant. The selection of design parameters is produced by solving a set of the LMI.

LMI theory has recently gained great attention since a wide variety of control problems can be reduced to a few standard convex optimization problems including LMIs. Consequently, optimisation problems with convex objective functions and LMI constraints are solvable relatively efficiently with off-the-shelf software. The form of an LMI is very general. Linear inequalities, convex quadratic inequalities, matrix norm inequalities, and various constraints from control theory, such as Lyapunov and Riccati inequalities, can be all be written as LMI. Thus, LMIs are a useful tool for solving a wide variety of optimisation and control problems [20], so LMI was adapted in this paper to obtain a gain for the observer design.

This paper presents a real-time system identification algorithm to determine the nonlinear parameters of an AUV dynamic model utilising the RLS. The identified real-time dynamic model coefficients allowed the AUV model to keep up with the information flow and to be continuously updated in response to the operational environment. Moreover, the high-gain observer based on the AUV dynamic model was developed to estimate the vehicle velocities through the water flow which were only intermittently unavailable from the DVL when the vehicle was operating in the midwater zone. The current velocities were consequently determined by using the estimated vehicle velocities through the water flow which let the AUV control and navigation system know the current velocities around the vehicle body.

This paper is organised as follows: Section II is devoted to clarify the methodology including the details of the instrumentation, AUV dynamics modelling and high-gain observer development. Results are presented in Section III and conclusions in Section IV.

II. METHDOLOGY

The water current velocity can be obtained from the difference between the vehicle velocity over the ground and the vehicle velocity through the water as illustrated simply in 1-D in Figure 2.

In this study, the current components close to the AUV were obtained in 3-principal directions by calculating the differences between the vehicle velocities over the ground measured by the DVL-aided INS during the field test and the vehicle velocities through the water estimated by using the AUV model-based high-gain observer. Equation (1) gives this calculation in the vector form.

$$\vec{v}_{Current} = \vec{v}_{OG} - \vec{v}_{TW} \tag{1}$$

where $\vec{v}_{Current}$ is the current velocity vector; $\vec{v}_{OG}$ is the vector of the vehicle's absolute velocity over the ground measured from field test using DVL-aided INS; and $\vec{v}_{TW}$ is the vector of vehicle's relative velocity through the water column obtained from AUV dynamic model.

During the field tests, the AUV underwent a straight-line, constant altitude mission while the water current velocities were measured through the AUV-onboard ADCP. The ADCPs were programmed to profile approximately 10 m of water column in 0.5 m range bins. The closest bin was 0.44 m away from the vehicle which referred as a blanking distance. Then water velocity components relative to the AUV in the body-fixed coordinate system in 3D were measured in each bin.

In order to analyse the motion of the AUV in 6 DOF, two coordinate frames, an inertial reference frame $\{x_i, y_i, z_i\}$ and a body-fixed frame $\{x_b, y_b, z_b\}$, were defined as indicated in Figure 3. While the Earth-fixed frame was used as the inertial reference, the body-fixed reference frame was fixed to the AUV. The origin O of the body-fixed reference frame was chosen at the centre of buoyancy of the vehicle.

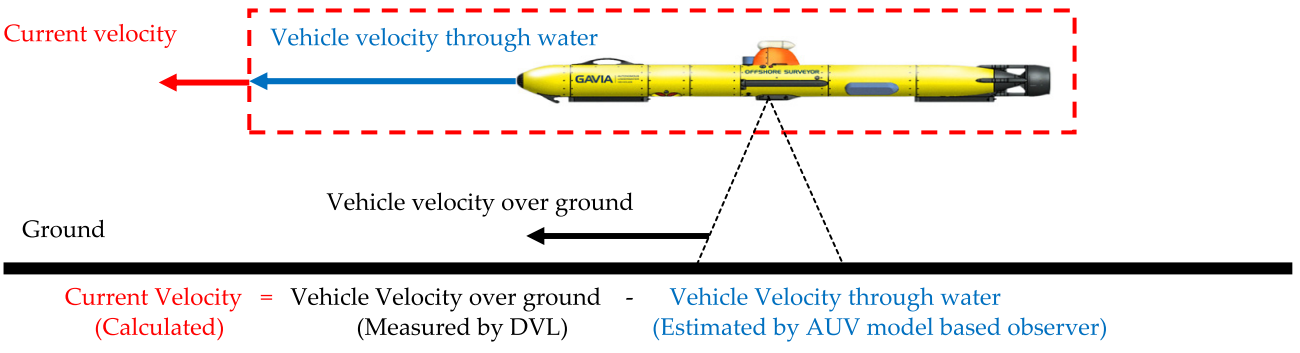

FIGURE 2. Illustration of current velocity, vehicle velocity through water and over ground.

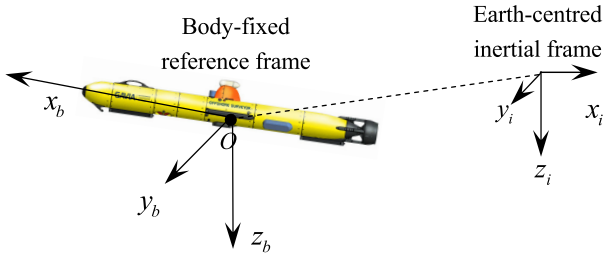

FIGURE 3. Body-fixed reference frame (LEFT) and Inertial Earth-centred inertial frame (RIGHT).

Without current compensation, the AUV control system only provides commands to keep the AUV on a straight-line motion in the absence of current. However, the truth is that the vehicle is also moving under the current disturbances. In this case, the vehicle cannot keep the desired straight-line trajectory within the given control inputs. Thus, the motion difference can be used for current estimation. In order to compensate for the disturbances caused by any turbulent or unsteady flow and keep the prescribed straight-line path, the AUV's control system is required to control the propeller RPM and control surface angles. These control commands were recorded in the vehicle log and used as inputs for the AUV model-based observer to estimate the AUV velocities through the water. As a result of the estimation, the current velocities could be determined by calculating the differences between the vehicle velocities over the ground recorded through DVL-aided INS and the estimated vehicle velocities through the water. This process of current estimation is illustrated as a flow chart in Figure 4.

A. VEHICLE SPECIFICATIONS

In order to validate the performance of the AUV model based observer for current estimation, field tests from a Gavia-class modular AUV were used. Its configuration is shown in Figure 5. The AUV consisted of a nose cone, battery module, interferometry sonar module (GeoSwath Plus Kongsberg Maritime AS), 1200 kHz Teledyne RD Instruments, ADCP/DVL module, Kearfott T24 INS module, control module and a propulsion module. The overall length of the vehicle was 2.7 m, the diameter was 0.2 m, and the dry weight in air was approximately 70 kg. The DVL-aided INS was used to derive the position of the AUV [10].

In the ADCP module, there were two 1200 kHz Teledyne RD Instruments ADCPs/DVLs which were installed in upward-looking and downward-looking configurations respectively. Both the upward-looking and downward looking transducers could collect water column velocity data relative to the AUV (i.e., in ADCP mode), but the downward-looking transducers could also measure the vehicle velocity over the ground (i.e., in DVL mode).

The aim of this study was to validate the applicability of the AUV model based high-gain observer for current estimate by comparing the measured vehicle velocities over ground and the estimated vehicle velocities relative to the water column

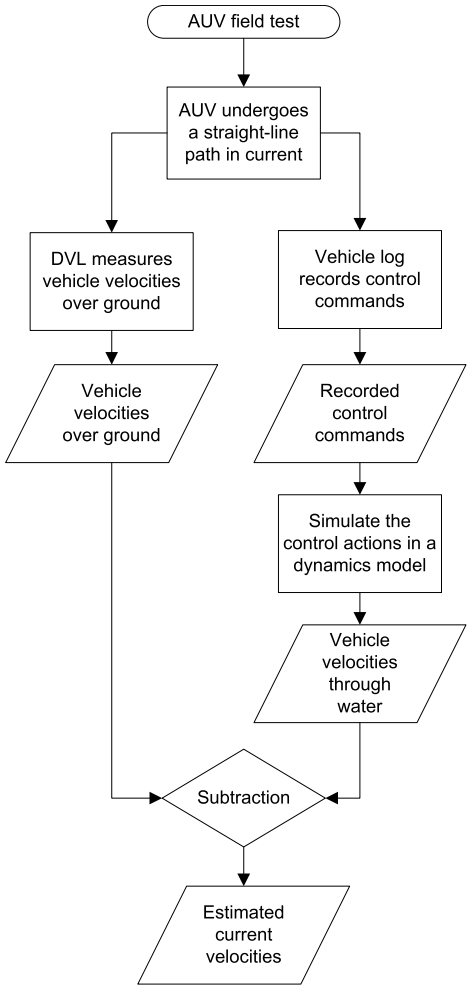

FIGURE 4. Flowchart to predict current velocities.

from an AUV model based high-gain observer. Consequently, the estimated current velocities are compared and validated by the current velocity measurements from the on-board ADCP. The field test was conducted in the Tamar estuary where there was a dominant tidal current flow and a straight-line run was conducted against the flow direction. Test details are published by Randeni *et al.* [10].

B. AUV DYNAMICS MODEL

The rigid body dynamics and hydrodynamics of the Gavia AUV were modelled according to the method formulated by Fossen [21] using MATLAB Simulink software. Referring to Fossen [21], the 6-DOF motion of an underwater vehicle can be expressed by Equation (2) and the mathematical equations in this paper are based on the notation as given in Table 1.

$$M\dot{v} + C(v)v + D(v)v + g(\eta) = t_{control}$$
$$M = M_{RB} + M_A \quad C(v) = C_{RB}(v) + C_A(v) \qquad (2)$$

where M is the system inertia matrix; C $(\boldsymbol{v})$ is the Coriolis-centripetal matrix; D $(\boldsymbol{v})$ is the damping matrix; $g(\eta)$ is the vector of the gravitational/buoyancy forces and moments; $t_{control}$ is the vector of body forces and moments; $\boldsymbol{v}$ is the

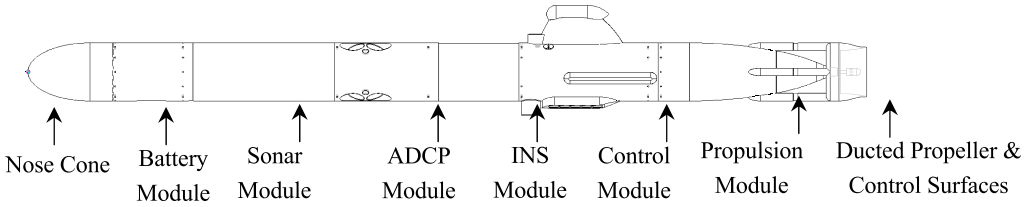

FIGURE 5. Configuration of the tested Gavia AUV

velocity vector (i.e., [u v w p q r] where p, q and r are the angular velocities around the x, y and z axes); η is the vector of position/Euler angles (i.e., [$xyz\varphi\theta\psi$]) where φ, θ and ψ are the roll, pitch and yaw angles respectively; M_{RB} is the rigid-body inertia matrix, $C_{RB}(\boldsymbol{\nu})$ is the rigid-body Coriolis and centripetal matrix, and finally M_A and $C_A(\boldsymbol{\nu})$ are their added mass components.

TABLE 1. The 6-DOF notation for marine vessels.

Degree-of-Freedom	Forces & Moments	Linear & Angular Velocity	Position & Euler Angles
Motions in the x-direction (surge)	X	u	x
Motions in the y-direction (sway)	Y	v	y
Motions in the z-direction (heave)	Z	w	x
Rotation about the x–axis (roll)	K	p	φ
Rotation about the y–axis (pitch)	M	q	θ
Rotation about the z–axis (yaw)	N	r	ψ

In response to the time series of control commands, the vehicle velocities through the water were reproduced by developing a motion model including inputs of propeller rotational rate (N), pitch angle (θ), pitch rate(q), pitch acceleration ($\dot{q}$), yaw rate (r) and yaw acceleration ($\dot{r}$). Instead of deriving the rolling, pitching and yawing motions, these were directly given as model inputs which allowed the mathematical model to be simplified to 3-DOF (i.e. into linear motions along the x, y and z directions) without modelling the angular motions.

In this study, Equation (2) which represents the 6-DOF dynamic equation of motion was reduced to 3-DOF and simplified by assuming:

Assumption: Products of inertia (i.e., I_{xy}, I_{xz} and I_{yz}) are assumed to be zero since they are negligibly small compared to the moments of inertia (i.e., I_{xx}, I_{yy} and I_{zz}) of the vehicle [22].

Then Equation (2) can be expanded and rearranged as:

$$\begin{aligned}&(m - X_{\dot{u}})\,\dot{u} + mz_g\dot{q} + my_g\dot{r}\\ &\quad = (W - B)\sin(\theta) + X_{u|u|}u|u| + \left(X_{wq} - m\right)wq\\ &\qquad + \left(X_{qq} + mx_g\right)q^2 + (X_{vr} + m)\,vr + \left(X_{rr} - mx_g\right)r^2\\ &\qquad + X_n \times N^2 \end{aligned} \tag{3}$$

$$\begin{aligned}&(m - Y_{\dot{v}})\,\dot{v} + \left(mx_g - Y_{\dot{r}}\right)\dot{r}\\ &\quad = Y_{v|v|}v|v| + Y_{r|r|}r|r| + (Y_{ur} - m)\,ur + Y_{uv}uv + mz_gqr \end{aligned} \tag{4}$$

$$\begin{aligned}&(m - Y_{\dot{w}})\,\dot{w} - \left(mx_g + Z_{\dot{q}}\right)\dot{q}\\ &\quad = (W - B)\cos(\theta) + Z_{w|w|}w|w| + Z_{q|q|}q|q|\\ &\qquad + \left(Z_{uq} + m\right)uq + Z_{uw}uw \end{aligned} \tag{5}$$

where, N is the propeller revolutions per minute (RPM) and X_n is the thrust coefficient, which is 95×10^{-6} for the Gavia AUV according to the estimation by Porgilsson [23]. The acceleration terms in the equations of motion were separated on the left-hand side while the right-hand sides included the hydrostatic, hydrodynamic damping and control forces.

$$\begin{aligned}&\dot{u} - X_n \times N^2\\ &\quad = \alpha_1\dot{q} + \alpha_2\dot{r} + \alpha_3 u|u| + \alpha_4 wq + \alpha_5 q^2\\ &\qquad + \alpha_6 vr + \alpha_7 r^2 + \alpha_8\sin(\theta) \end{aligned} \tag{6}$$

$$\dot{v} = \beta_1\dot{r} + \beta_2 v|v| + \beta_3 r|r| + \beta_4 r^2 + \beta_5 ur + \beta_6 uv + \beta_7 qr \tag{7}$$

$$\begin{aligned}&\dot{w} = \gamma_1\dot{q} + \gamma_2 w|w| + \gamma_3 q|q| + \gamma_4 uq + \gamma_5 uw + \gamma_6 q^2\\ &\qquad + \gamma_7 rq + \gamma_8\cos(\theta) \end{aligned} \tag{8}$$

The coefficients (e.g., m, $X_{\dot{u}}$ and z_g) in Equations (3) - (5) were superimposed in unknown parameters (α_{1-8}, β_{1-7} and γ_{1-8}) in Equation (6) - (8), which eliminated the need to measure them. While the vehicle's linear accelerations (i.e., $\dot{u}$, $\dot{v}$ and $\dot{w}$) were rearranged on the left hand sides of Equation (6) - (8), unknown parameters on the right hand sides were to be identified by using the Recursive Least Squares (RLS) algorithm approach.

In Equation (9), the system output vector $\mathrm{y}_{(t)}$ was comprised of a regressor vector $\Gamma_{(t)}$ and a parameter vector $\Phi_{(t)}$, and accordingly Equation (6) - (8) were represented in TABLE 2.

$$y_{(t)} = \Gamma_{(t)}\Phi_{(t)} \tag{9}$$

In highly dynamic environments, the parameters of the mathematical model fluctuate with time due to environmental forces [2]. Therefore, in this study, a real-time model identification algorithm was utilised to identify the dynamics parameters with continuous updates, which allowed the AUV model to produce the vehicle's motion response in the present environment.

Unknown parameter vectors were identified in real-time by utilising the Recursive Least Squares (RLS) estimation

TABLE 2. $y_{(t)}$, $\Gamma_{(t)}$ and $\Phi_{(t)}$ Vectors for Representation of Equation (6) - (8).

Axis	Outcome, $y_{(t)}$	Regressor, $\Gamma_{(t)}$	Parameter, $\Phi_{(t)}$
x	$\dot{u}\text{-}X_{\eta}N^2$	$\begin{bmatrix}\dot{q} & \dot{r} & u\lvert u\rvert & wq & q^2 & vr & r^2 & \sin(\theta)\end{bmatrix}$	$\begin{bmatrix}\alpha_1 & \alpha_2 & \alpha_3 & \alpha_4 & \alpha_5 & \alpha_6 & \alpha_7 & \alpha_8\end{bmatrix}$
y	$\dot{v}$	$\begin{bmatrix}\dot{r} & v\lvert v\rvert & r\lvert r\rvert & r^2 & ur & uv & qr\end{bmatrix}$	$\begin{bmatrix}\beta_1 & \beta_2 & \beta_3 & \beta_4 & \beta_5 & \beta_6 & \beta_7\end{bmatrix}$
z	$\dot{w}$	$\begin{bmatrix}\dot{q} & w\lvert w\rvert & q\lvert q\rvert & uq & uw & \cos(\theta)\end{bmatrix}$	$\begin{bmatrix}\gamma_1 & \gamma_2 & \gamma_3 & \gamma_4 & \gamma_5 & \gamma_6 & \gamma_7 & \gamma_8\end{bmatrix}$

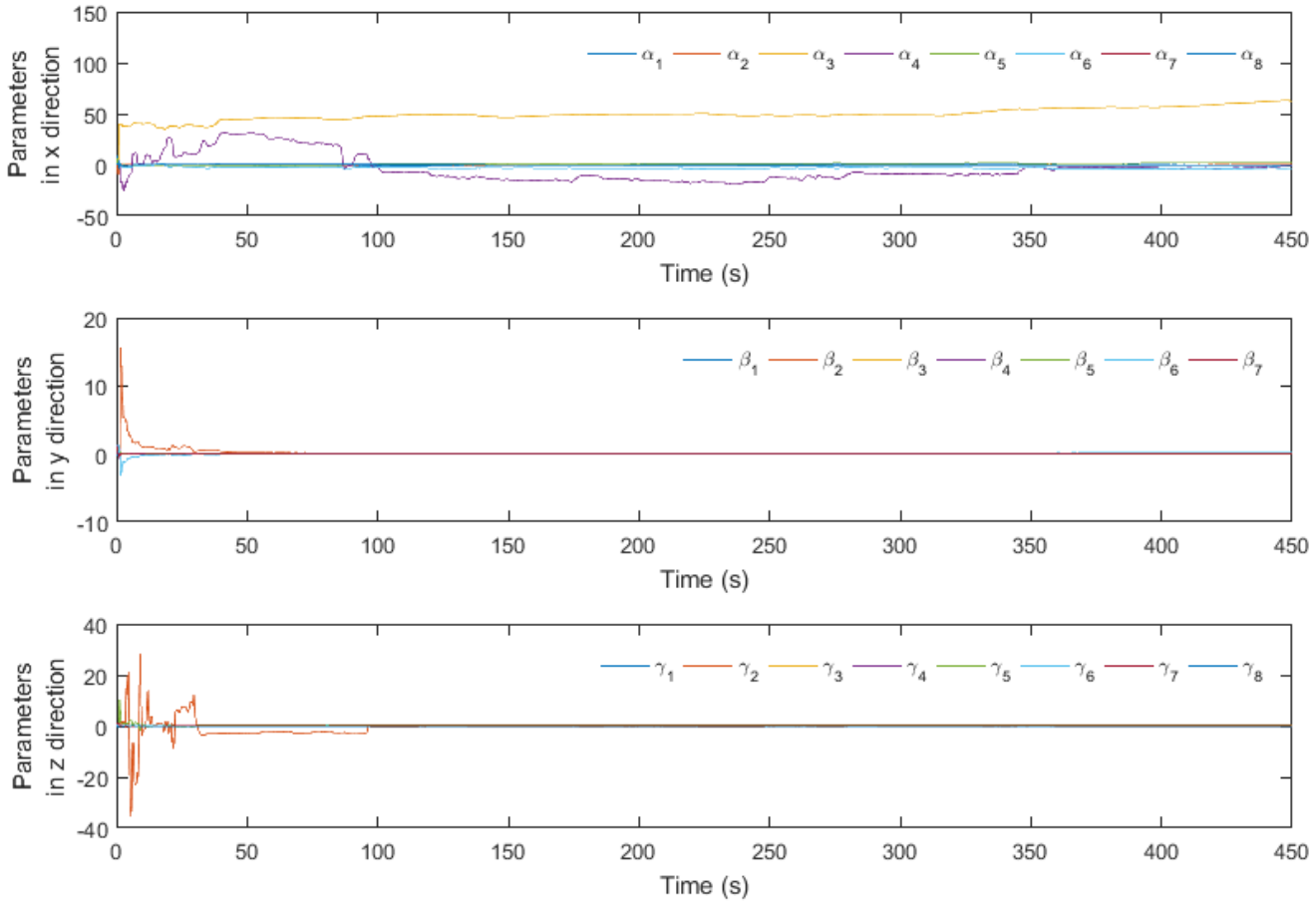

FIGURE 6. Dynamics model parameters identified by the real-time RLS method during the simulation

TABLE 3. Identified parameter values at the end of simulation.

	1	2	3	4	5	6	7	8
$\alpha_{1\text{-}8}$	-0.3335	0.0699	62.5408	-1.8373	1.8108	-3.3354	0.0856	33.3374
$\beta_{1\text{-}7}$	-0.0120	-0.0250	-0.0022	0.0012	0.0500	0.1757	0.0012	-
$\gamma_{1\text{-}8}$	0.0129	-0.1582	-0.0042	-0.0196	0.4036	0.0004	0.0003	-0.0096

block set up in the MATLAB Simulink Identification toolbox. The identified parameters were varied while the simulation was running as shown in Figure 6, and parameters at the end of simulation, for example, are tabulated in TABLE 3.

In order to obtain the AUV's linear velocities, the linear acceleration terms from Equation (6)- (8) were solved in the AUV dynamics model by using the recorded input values as shown in the flow chart in Figure 7. Six inputs were recorded, such as: propeller rotation rate (N), pitch angle (θ), pitch rate (q), pitch acceleration ($\dot{q}$), yaw rate (r) and yaw acceleration ($\dot{r}$). Integrating the linear accelerations with respect to time produced the linear velocities in the body-fixed reference frame.

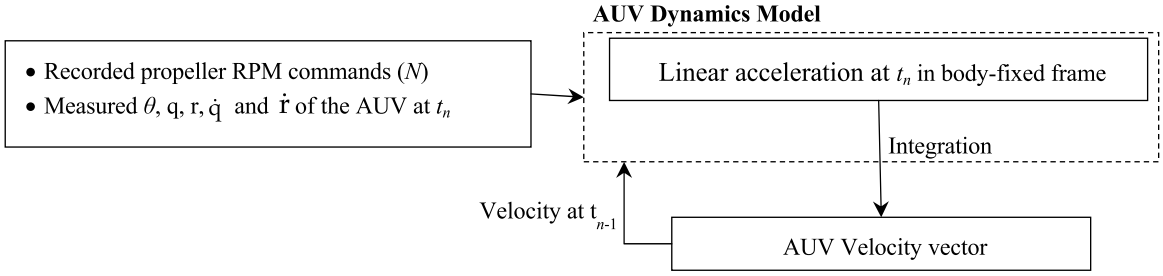

FIGURE 7. Model-based velocity calculation flowchart. The acceleration at $t_n t_n$ was obtained with recorded RPM (N), measured variables (θ, q, r, $\dot{q}$ and $\dot{r}$) as well as velocity vector at $t_{n-1} t_{n-1}$. Then AUV velocity vector is solved by integrating the acceleration vector with respect to time.

C. HIGH-GAIN OBSERVER DESIGN

In this section, a high-gain observer based on the AUV dynamics model was designed. In order to set up the nonlinear high-gain observer, the AUV's dynamic systems are described by:

$$\begin{aligned} \dot{x} &= Ax + f(x,t) \\ y &= Cx \end{aligned} \tag{10}$$

where $x \in \mathbb{R}^n$ is the state vector; $y(t) \in \mathbb{R}^m$ is the measurement output vector; and, $A \in \mathbb{R}^{n\times n} C \in \mathbb{R}^{m\times n}$, and the function f are defined as follows:

$$x(t) = [\ \phi \quad \theta \quad \psi \quad u_r \quad v_r \quad w_r\ ]^T$$

$$C = \begin{bmatrix} 0 & 0 & 0 & 1 & 0 & 0 \\ 0 & 0 & 0 & 0 & 1 & 0 \\ 0 & 0 & 0 & 0 & 0 & 1 \end{bmatrix}$$

$$f(x,t) := \begin{bmatrix} f_1(x_1,t) \\ f_2(x_1,x_2,t) \\ \vdots \\ f_{n-1}(x_1,x_2,\ldots,x_{n-1},t) \\ f_n(x_1,x_2,\ldots,x_n,t) \end{bmatrix}$$

To estimate $x(t)$, the observer was considered as follows:

$$\dot{\hat{x}} = A\hat{x} + \hat{f}(\hat{x},u) + G(\gamma)(y - C\hat{x}) \tag{11}$$

where $\hat{x}(t)$ is the estimate of $x(t)$ at time t; the observer gain, $G(\gamma, K) := [\gamma k_1 \gamma^2 k_2 \ldots \gamma^n k_n]^T$ with $K := [k_1 k_2 \ldots k_n]^T$ and $k_i \in \mathbb{R}$, $i = 1, 2, \ldots, n$. [19]. The estimation error $\left(\hat{e} := x - \hat{x}\right)$ dynamics were derived from Equation (10) and (11) as follows:

$$\dot{\hat{e}}(t) = (A - GC)\,\hat{e}(t) + f(x(t),t) - \hat{f}(x(t) - \hat{e}(t),t) \tag{12}$$

Instead of studying the stability of the estimation error, variables were transformed $\hat{e} := T(\gamma)e$, $e \in \mathbb{R}^n$ with $T(\gamma) = diag\left(\gamma, \gamma^2, ..., \gamma^n\right)$ resulting Equation (13) as follows:

$$\begin{aligned} \dot{e}(t) &= T(\gamma)^{-1}(A - GC)T(\gamma)e(t) \\ &\quad + T(\gamma)^{-1}\left\{f(x(t),t) - f(x(t) - T(\gamma)e(t),t)\right\} \end{aligned} \tag{13}$$

Because of the particular observer structure, the previous equation was rewritten as follows:

$$\begin{aligned} \dot{e}(t) &= \gamma(A - KC)e(t) \\ &\quad + T(\gamma)^{-1}(f(x(t),t) - f(x(t) - T(\gamma)e(t),t)) \end{aligned} \tag{14}$$

The stability of the error dynamics was investigated via a Lyapunov function. Furthermore, based on the fact that (A, C) is observable, there exist $\lambda > 0, K \in \mathbb{R}^n$ and a symmetric positive matrix $P \in \mathbb{R}^{n\times n}$ such that

$$(A - KC)^{\mathrm{T}} P + P(A - KC) + \lambda I < 0 \tag{15}$$

with $K := [k_1\ k_2 \cdots k_n]^T$. The above equation could be treated by solving the equivalent LMI:

$$A^{\mathrm{T}}P + PA - C^{\mathrm{T}}Y^{\mathrm{T}} - YC + \lambda I < 0 \tag{16}$$

where the unknowns are $\lambda > 0$, $Y = PK \in \mathbb{R}^n$ and $P > 0$.

In order to compute the solution to a given system of LMIs, a number of MATLAB functions were used as tabulated in Table 4. Before starting the description of a new LMI system, a function `setlmis` was used to initialise its internal representation. The function `limvar` defined new matrix variables P, Y and λ in the LMI system currently described. The variable matrix P was defined as a 6×6 symmetric matrix while Y was defined as a 6×3 rectangular matrix. One of the gain parameters, λ was defined as a constant. By using a function `limterm`, the term contents of an LMI one term at a time. The LMI term referred to the elementary additive terms involved in the block-matrix expression of the LMI. For example, in order to express the Equation (16), three terms were required as shown in TABLE 4. For more details for the `lmiterm` function description, see [24]. After completing the description of a given LMI system with `lmivar` and `lmiterm`, its internal representation `lmisys` was obtained with the command `getlmis`. The function `feasp` computed a solution `xfeas` of the system of LMIs descripted by `lmisys`. The vector `xfeas` was a particular value of the decision variables for which all LMIs were satisfied. Finally, a function `dec2mat` computed the corresponding value `valx` of the matrix variable with identifier X given the value `decvars` of the vector of decision variables. As a result, matrix variables – P, Y and λ in the LMI system were obtained, then P and Y were used to calculate the one of gain parameter K.

The high-gain observer design was accomplished by solving the LMI problem so the gain $K = P^1 Y$ and γ were

TABLE 4. Matlab functions used to find the gain matrix and its description [24].

	MATLAB function	Function description
1	`setlmis([])`	Initialize description of LMI system
2	`lmivar(type,struct)` Type = 1: Symmetric matrices with a block-diagram structure. Type = 2: Full *m-by-n* rectangular matrix.	Specify matrix variables in LMI problem.
	`P=lmivar(1,[6 1])`	Specify matrix P (6×6)
	`Y=lmivar(2,[6 3])`	Specify matrix Y (6×3)
	`lambda=lmivar(1,[1 1])`	Specify matrix λ (1×1)
3	`lmiterm(termID,A,B,flag)`	Specify term content of LMIs
	`lmiterm([1 1 1 P],1,A,'s')`	$A^{\mathrm{T}}P+PA$
	`lmiterm([-1 1 1 Y],1,C,'s')`	$C^{\mathrm{T}}Y^{\mathrm{T}}+YC$
		$A^{\mathrm{T}}P+PA-C^{\mathrm{T}}Y^{\mathrm{T}}-YC+\lambda I<0$
	`lmiterm([1 1 1 lambda],1,1)`	λI
	`lmiterm([-2 1 1 P],1,1)`	$P>0$
	`lmiterm([-3 1 1 lambda],1,1)`	$\lambda>0$
4	`lmisys=getlmis`	Internal description of LMI system.
5	`[tmin,xfeas]=feasp(lmisys)`	Compute solution (xfeas) to given system of LMIs.
6	`valX=dec2mat(lmisys,decvars,X)`	Given values of decision variables, derive corresponding values of matrix variables.
	`P=dec2mat(lmisys,xfeas,P)`	Solution for Matrix P
	`Y=dec2mat(lmisys,xfeas,Y)`	Solution for Matrix Y
	`lambda=dec2mat(lmisys,xfeas,lambda)`	Solution for Matrix λ
7	`K=inv(P)*Y;`	Calculation of the gain matrix K .

obtained as follows:

$$\gamma = 2.2707, \quad K = \begin{bmatrix} 1.3383 & 0 & 0.8730 \\ 0 & 0.7599 & 0 \\ 0.2967 & 0 & 0.8041 \\ 0 & 0.1586 & 0 \\ 0.5121 & 0 & 0.7589 \\ 0 & -0.1884 & 0 \\ -8.0381 & 0 & 34503 \\ 0 & 2.1625 & 0 \\ 3.2320 & 0 & 3.6946 \end{bmatrix}$$

III. RESULTS AND DISCUSSION

The proposed high-gain observer design was validated by comparing the estimated current velocities with recorded current velocities from an on-board ADCP. In the field test, the AUV underwent a straight and constant depth mission as illustrated in Figure 8 and Figure 9 respectively.

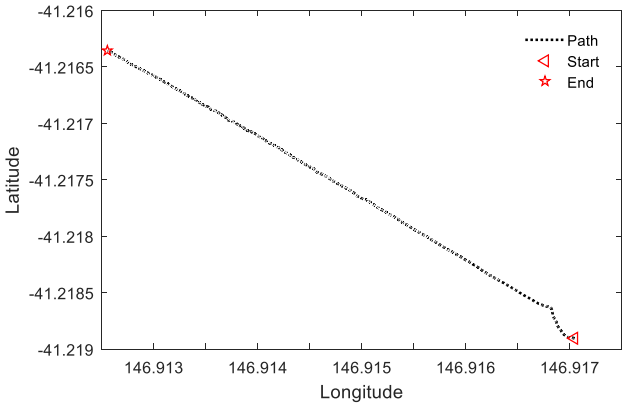

FIGURE 8. Trajectory that the vehicle underwent during the field test

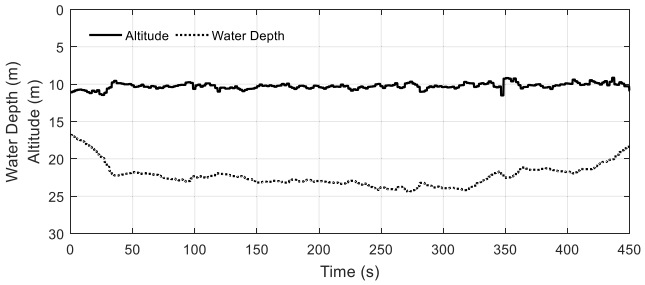

FIGURE 9. **Water Depth and AUV's altitude during the field test**

In order to estimate the current velocities, firstly the vehicle's velocities through the water were estimated by the model-based observer. Then the current velocities could be calculated by subtracting the estimated velocities through the water from the vehicle's velocities over the ground measured by the DVL.

Figure 10 shows the vehicle's velocities over the ground recorded by the DVL-aided INS navigation system during the field test and vehicle's velocities through the water estimated by the model-based observer in the x_b, y_b and z_b direction respectively. In the x_b axis, the vehicle velocities over the ground and through the water showed the greatest difference compared to those in they_b and z_b axes. This difference leads to an estimate of around -1 m/s current velocity in the longitudinal direction. It can be inferred that the straight line that the vehicle followed during the field test was against the tidal flow direction.

Figure 11 shows the current velocities estimated by the AUV model-based observer and measured current velocities from the ADCP in the x_i, y_i and z_i axes directions, respectively. Although the current velocities were measured 0.44 m away from the vehicle due to the ADCP's blanking distance, the estimated current velocities from the observer were closely matched with the measured current velocities. A peaking phenomenon was found in the estimated current velocity especially in the x_i axis as shown in Figure 12. Using the high-gain observer results in a peaking phenomenon which shows up as a large estimation gap during the short period right after the initial time. However, the transient period shown in the estimated current velocity was very short relative to the time scale, and the estimated velocities approached the measured current velocities very promptly and closely.

In order to investigate the differences between the current velocity estimates from the AUV model-based observer and the current velocities measured by the ADCP, the standard deviations between these two were quantified in Table 5. Here, the standard deviation of the current estimate results were 0.0942 m/s, 0.0656 m/s and 0.0323 m/s. The current measurement from the ADCP were taken 0.44 m away from the vehicle while the current estimates from the observer were calculated at the vehicle.

In the research of Randeni *et al.* [10], a method is proposed to calculate the water velocity components of a turbulent water column using the AUV motion response (referred to

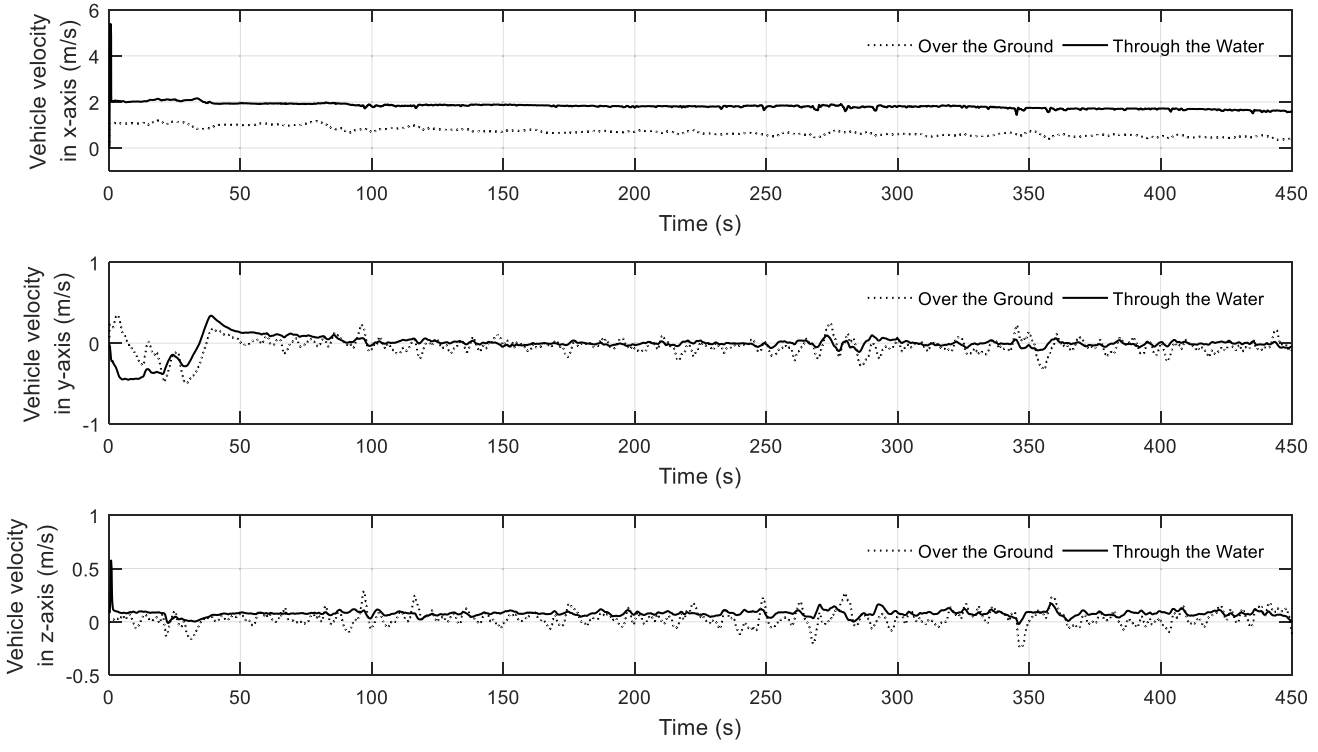

FIGURE 10. **The vehicle velocities over ground measured by DVL-aided INS (dotted curves) and velocities through water estimated by AUV model-based high-gain observer (solid curve) along x, y and z axis.**

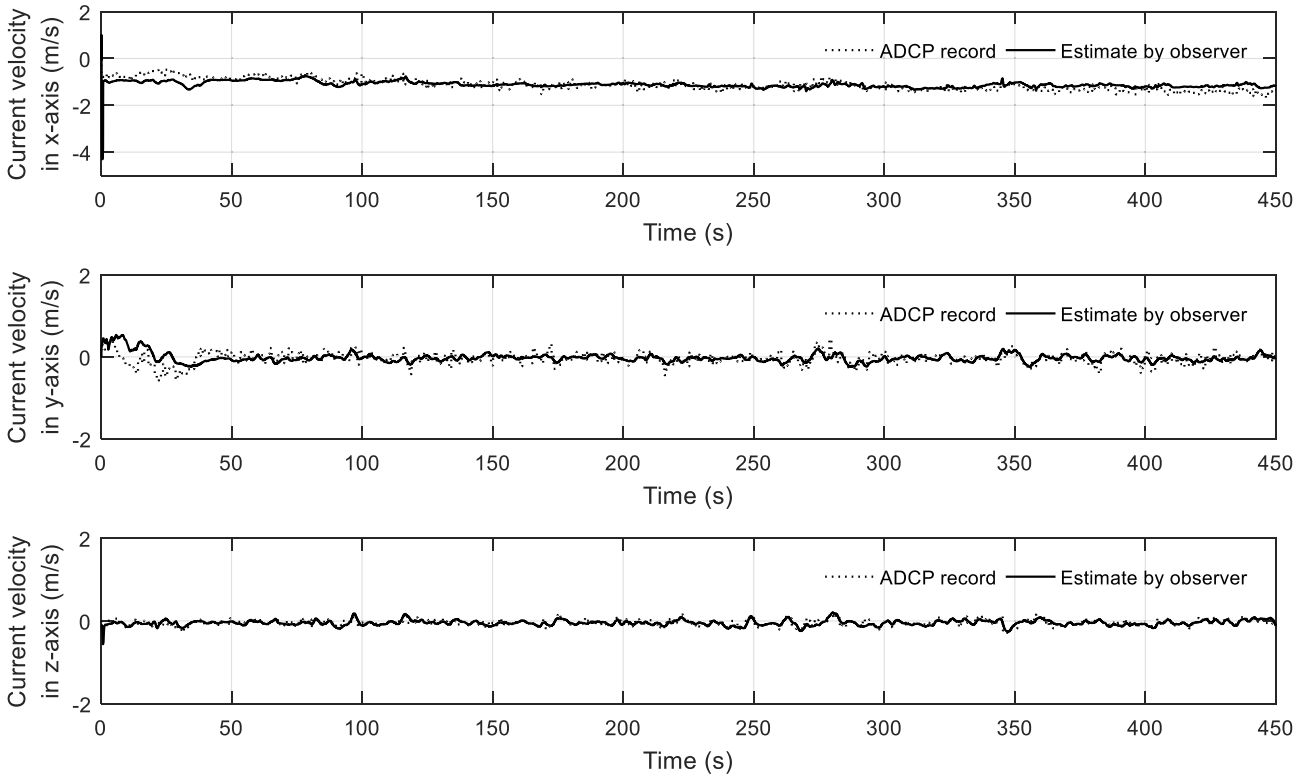

FIGURE 11. The comparison between the current velocities measured by ADCP (dotted curve) and its counterpart which was estimated by the high-gain observer (solid curve) in x, y and z axis.

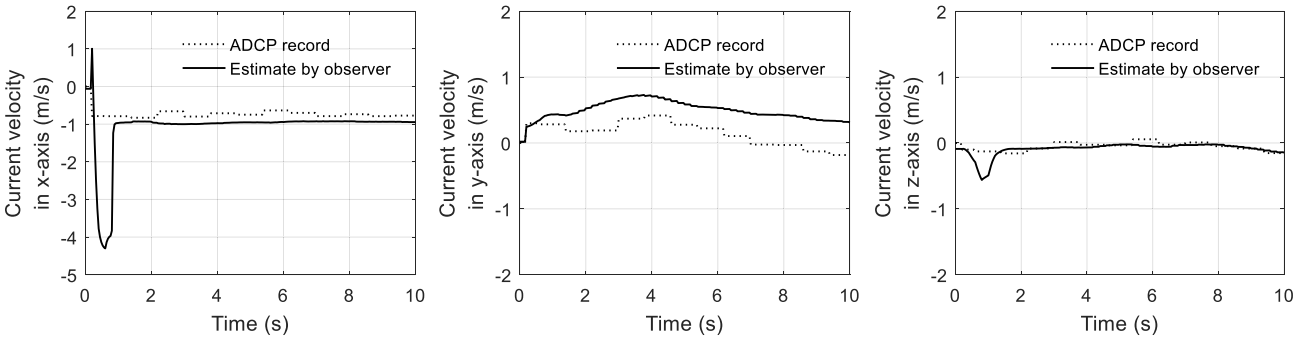

FIGURE 12. Peaking phenomena in current estimation at the beginning of the estimation process (∼ 10 second) compared to the current velocities recorded by the ADCP.

TABLE 5. Standard deviation of current estimates.

Direction	x - axis	y - axis	z - axis
Standard Deviation	0.0942 m/s	0.0656 m/s	0.0323 m/s
Absolute error	0.108 m/s	0.067 m/s	0.030 m/s

as the 'WVAM method'), for which the current velocities are solved by determining the difference between the motion responses of the vehicle in calm and turbulent water environments. The field test data used in this study was acquired from part of the Randeni *et al.* [10] study, which allowed a comparison to be made between the respective methods for current velocities estimation. Figure 13 shows the comparison between the current measurements from the ADCP, the current velocity estimated from the AUV model-based observer and the current velocity calculated by WVAM method in three dimensions.

The difference between velocities obtained from the WVAM method and ADCP were calculated by quantifying the standard deviation and these are 0.09 m/s, 0.07 m/s and 0.06 m/s [10]. Compared with the standard deviation of the current estimate results using the high-gain observer, those for the x_i and y_i axes were similar, but the standard deviation of the current estimation from the high-gain observer in the z_i axis was less: 0.0323 m/s.

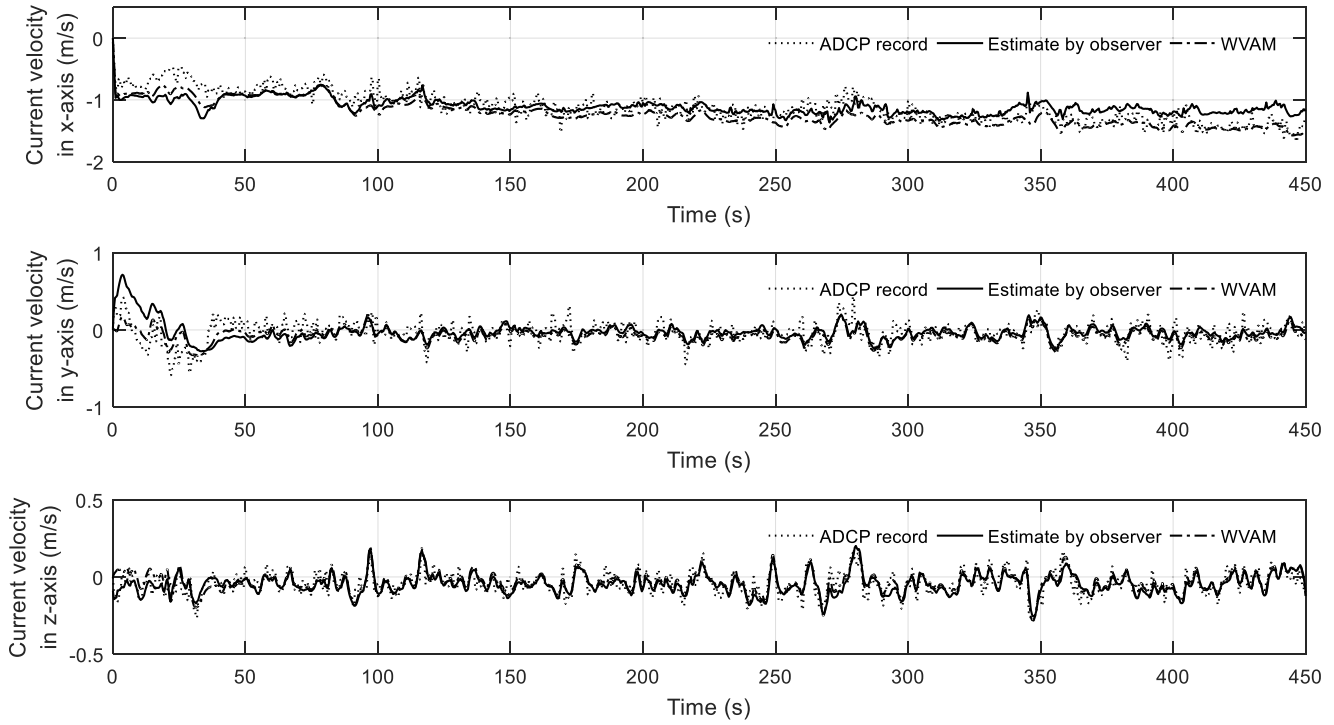

FIGURE 13. Comparison between the current velocities in the z direction between ADCP measurement, estimate from the observer and calculation from WVAM method respectively.

Furthermore, an estimate of error was calculated by using equation (17) to assess the improvement of the proposed AUV model-based observer to estimate the current velocity compared with the WVAM method.

$$estimationerror(\%) = (V_{ADCP} - V_{Est})/V_{ADCP} \times 100 \quad (17)$$

where V_{ADCP} is the measured current velocity by ADCP and V_{Est} is the estimated current velocity by the observer and the WVAM method.

In TABLE 6, estimation error means of the current estimation results for the model-based observer and WVAM method are tabulated. The estimation error means of the model-based observer was smaller than their counterpart from the WVAM method in both x_i and z_i axes which results in an estimation improvement of 4.992 % and 6.757 % respectively. In the y_i axis, the estimation error mean of the model-based observer was slightly larger than its counterpart from the WVAM method. This could have resulted from a lower number of unknown parameters (β_{1-7}) in the y_i axis dynamic equation than the number of parameters in the other two axes (α_{1-8} and γ_{1-8}), while the number of the unknown parameters of each axis had been decided by rearranging and superimposing of the underactuated AUV dynamic motion equation. This could have resulted in the current estimation in y_i axis converged into the measured current velocity more slowly than the other two axes, as is shown in the time period between 0 to 50 second in Figure 13, which caused the slightly larger estimation error mean in the y_i axis than the counterpart of WVAM method.

TABLE 6. Estimation error mean for model-based observer and wvam method.

Estimation Error Mean (%)	x_i axis	y_i axis	z_i axis
Model-based observer	1.222 %	0.810 %	0.370 %
WVAM method	1.283 %	0.778 %	0.395 %
Estimation improvement of model-based observer	+4.992%	-3.951 %	+6.757 %

In contrast to the WVAM method, estimated current velocities using the AUV model-based observer did not require an additional field test in a calm water environment in order to reproduce the AUV responses in the simulation model.

IV. CONCLUSION

In order to verify the capability of the AUV dynamic model-based observer for predicting the water current velocities in this study, the water current velocity components in the x_i, y_i and z_i axes of inertial frame were estimated. The water current velocities were estimated by calculating the difference between the vehicle velocities over ground recorded using the DVL and the vehicle velocities through the water estimated from an AUV model-based observer. A Gavia AUV was utilised to conduct a straight-line, constant depth mission to record the current velocities and vehicle velocities by

utilising on-board ADCP and DVL respectively. The AUV dynamics model that represents the Gavia AUV behaviour was developed using MATLAB Simulink. Instead of deriving the roll, pitch and yaw motions, these were directly given as simulation inputs which allowed the AUV dynamics model to be simplified to 3-DOF. For the AUV dynamic model, hydrodynamics parameters were identified by applying real-time system identification utilising the RLS identification method. The RLS identification technique was used as it has the advantages of simple calculation and good convergence properties. The real-time model identification algorithm allowed the AUV model to be continuously updated in response to the operational environment. The high-gain observer was used as a nonlinear estimation algorithm to obtain the vehicle velocities through the water. Stability of the estimation error dynamics was investigated via the Lyapunov function. The observer gain was computed by solving the LMIs (Linear Matrix Inequalities) which represented the error dynamics equation.

During the AUV simulation, the vehicle velocities through the water were obtained by applying the equivalent control commands which were executed during the field test. Once the vehicle velocities through the water were available, the current velocities were calculated by subtracting the vehicle velocities through the water from the vehicle velocities over the ground recorded by the DVL-aided INS. The estimated current velocities in the x_i, y_i and z_i direction were found to be well matched with the measured current from the AUV-onboard ADCP. In order to quantify the differences between the estimated and measured current velocities, standard deviations were calculated as 0.0942 m/s, 0.0656 m/s and 0.0323 m/s for the x_i, y_i and z_i axes components respectively. Furthermore, the current estimation results from the AUV model-based observer were also compared with the estimation results from the WVAM method [10] which utilises motion differences. The estimation error percentages illustrated that the current estimation found by using the model-based observer was improved by as much as 6.8 % in the z_i axis, less in the other directions.

For precise navigation and control of an AUV, it is critical to obtain the current velocities around the boundary layer of the AUV where the ADCP is unable to measure due to its blanking distance. Hence the AUV model-based observer is advantageous to estimate the current velocities either close to or at the vehicle by utilising an AUV dynamics model. Precise hydrodynamics properties can be identified from the real-time measurement.

ACKNOWLEDGMENT

The authors thank Supun Randeni (Postdoctoral Research Associate at Massachusetts Institute of Technology) and Alexander Forrest (Assistant Professor at University of California - Davis) for conducting the AUV field experiments and allowing us to use the data set for this study.

REFERENCES

[1] L. Medagoda, S. B. Williams, O. Pizarro, and M. V. Jakuba, "Water column current aided localisation for significant horizontal trajectories with autonomous underwater vehicles," in *Proc. OCEANS MTS/IEEE KONA*, Sep. 2011, pp. 1–10.
[2] P. S. Randeni, A. L. Forrest, R. Cossu, Z. Q. Leong, D. Ranmuthugala, and V. Schmidt, "Parameter identification of a nonlinear model: Replicating the motion response of an autonomous underwater vehicle for dynamic environments," *Nonlinear Dyn.*, vol. 91, no. 2, pp. 1229–1247, Jan. 2018.
[3] M. Dinc and C. Hajiyev, "Integration of navigation systems for autonomous underwater vehicles," *J. Mar. Eng. Technol.*, vol. 14, no. 1, pp. 32–43, May 2015.
[4] O. Hegrenas, E. Berglund, and O. Hallingstad, "Model-aided inertial navigation for underwater vehicles," in *Proc. IEEE Int. Conf. Robot. Autom.*, May 2008, pp. 1069–1076.
[5] O. Hegrenæs and O. Hallingstad, "Model-aided ins with sea current estimation for robust underwater navigation," *IEEE J. Ocean. Eng.*, vol. 36, no. 2, pp. 316–337, Apr. 2011.
[6] S. A. T. Randeni P, Z. Q. Leong, D. Ranmuthugala, A. L. Forrest, and J. Duffy, "Numerical investigation of the hydrodynamic interaction between two underwater bodies in relative motion," *Appl. Ocean Res.*, vol. 51, pp. 14–24, Jun. 2015.
[7] X. Liang, Y. Li, Z. Peng, and J. Zhang, "Nonlinear dynamics modeling and performance prediction for underactuated AUV with fins," *Nonlinear Dyn.*, vol. 84, no. 1, pp. 237–249, Apr. 01 2016.
[8] Z. Yan, D. Wu, J. Zhou, and L. Hao, "Recursive subspace identification of AUV dynamic model under general noise assumption," *Math. Problems Eng.*, vol. 2014, Jan. 2014, Art. no. 547539.
[9] L. Ljung, *System Identification: Theory for the User* (Prentice-Hall Information and System Sciences Series), 2nd ed. Upper Saddle River, NJ, USA: Prentice-Hall, 1999.
[10] P. S. Randeni, A. Forrest, R. Cossu, Z. Leong, and D. Ranmuthugala, "Determining the horizontal and vertical water velocity components of a turbulent water column using the motion response of an autonomous underwater vehicle," *J. Marine Sci. Eng.*, vol. 5, no. 3, p. 25, 2017.
[11] K. Reif and R. Unbehauen, "The extended Kalman filter as an exponential observer for nonlinear systems," *IEEE Trans. Signal Process.*, vol. 47, no. 8, pp. 2324–2328, Aug. 1999.
[12] S. J. Julier and J. K. Uhlmann, "Unscented filtering and nonlinear estimation," *Proc. IEEE*, vol. 92, no. 3, pp. 401–422, Mar. 2004.
[13] J. Carpenter, P. Clifford, and P. Fearnhead, "Improved particle filter for nonlinear problems," *IEE Proc.-Radar, Sonar Navigat.*, vol. 146, no. 1, pp. 2–7, Feb. 1999.
[14] B. Zheng, P. Fu, B. Li, and X. Yuan, "A robust adaptive unscented Kalman filter for nonlinear estimation with uncertain noise covariance," *Sensors*, vol. 18, no. 3, p. 808, 2018.
[15] H. K. Khalil and L. Praly, "High-gain observers in nonlinear feedback control," *Int. J. Robust Nonlinear Control*, vol. 24, no. 6, pp. 993–1015, Apr. 2014.
[16] H. K. Khalil, "Cascade high-gain observers in output feedback control," *Automatica*, vol. 80, pp. 110–118, Jun. 2017.
[17] C. Tréangle, M. Farza, and M. M'Saad, "A simple filtered high gain observer for a class of uncertain nonlinear systems," in *Proc. 18th Int. Conf. Sci. Techn. Autom. Control Comput. Eng. (STA)*, Dec. 2017, pp. 396–401.
[18] S. Fan, W. Xu, Z. Chen, and F. Zhang, "Nonlinear observer design for current estimation based on underwater vehicle dynamic model," in *Proc. OCEANS-Shanghai*, Apr. 2016, pp. 1–5.
[19] A. Alessandri and A. Rossi, "Time-varying increasing-gain observers for nonlinear systems," *Automatica*, vol. 49, no. 9, pp. 2845–2852, Sep. 2013.
[20] J. G. VanAntwerp and R. D. Braatz, "A tutorial on linear and bilinear matrix inequalities," *J. Process Control*, vol. 10, no. 4, pp. 363–385, Aug. 2000.
[21] T. I. Fossen, *Handbook of Marine Craft Hydrodynamics and Motion Control*. Hoboken, NJ, USA: Wiley, 2011.
[22] T. Prestero, "Verification of a six-degree of freedom simulation model for the REMUS autonomous underwater vehicle," M.S. thesis, Dept. Ocean Eng., Massachusetts Inst. Technol., Cambridge, MA, USA, 2001.
[23] H. Porgilsson, "Control of a small undermanned underwater vehicle using zero optimizing controllers," M.S. thesis, Dept. Elect. Comput. Eng., Univ. Iceland, Reykjavík, Iceland, 2006.
[24] MathWorks. (2018). *LMI Applications*. [Online]. Available: https://au.mathworks.com/ help/robust/ug/lmi-applications.html?searchHighlight=lmi&s_tid=doc_srchtitle

EONJOO KIM received the B.E. degree in marine and offshore engineering from the Australian Maritime College, University of Tasmania, Launceston, Australia, in 2015, where she is currently pursuing the Ph.D. degree with the College of Sciences and Engineering. Her research interests include the navigation and control of autonomous underwater vehicles.

Dr. Kim was a recipient of the Australian Postgraduate Awards Program in 2017.

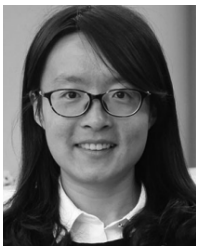

SHUANGSHUANG FAN (M'15) received the B.E. degree in mechanical engineering from Shandong University, Jinan, China, in 2008, and the Ph.D. degree in mechatronic engineering from Zhejiang University, Hangzhou, China, in 2013.

From 2013 to 2014, she was a Research Engineer with the Shanghai Aerospace Control Technology Institute, Shanghai, China. She was with the Acoustic Signal Processing Lab, Zhejiang University, as a Post-Doctoral Researcher, from 2014 to 2017. She is currently a Lecturer with the Australian Maritime College, University of Tasmania, Launceston, Australia. She is also an Adjunct Professor with the Department of Ocean and Naval Architectural Engineering, Memorial University of Newfoundland, St. John's, Canada.

Her research interests include the navigation, control, and path planning of underwater vehicles in dynamic environments.

NEIL BOSE received the B.Sc. degree in naval architecture and ocean engineering from the University of Glasgow in 1978 and the Ph.D. degree from the University of Glasgow in 1982.

He joined the Australian Maritime College (AMC) in 2007 as the Manager of the Australian Maritime Hydrodynamics Research Centre. He was also a Professor of maritime hydrodynamics with the AMC. From 2009 to 2011, he was the Director of the AMC's National Centre for Maritime Engineering and Hydrodynamics. He served as Principal for AMC, University of Tasmania, since 2012. He was appointed as the Vice-President (Research) at the Memorial University of Newfoundland, Canada, in 2017. He is currently an Adjunct Professor with AMC.

His research interests include marine propulsion, autonomous underwater vehicles, ocean environmental monitoring, ocean renewable energy, ice/propeller interaction, and aspects of offshore design.